J. Eng. Technol. Sci., Vol. 53, No. 1, 2021, 210103

Experimental Study and Numerical Model of Spruce and Teak Wood Strength Properties Under Compressive High Strain Rate Loading

Ediansjah Zulkifli*, Patria Kusumaningrum & Diah Puspita Rahmi

Civil Engineering and Environment Department, Bandung, Institut Teknologi Bandung, Jalan Ganesha No. 10, Bandung 40132, Indonesia
*E-mail: ednsjah@si.itb.ac.id

Highlights:

- The dynamic increase factor phenomenon occurred in both tested materials, soft wood and hard wood, with the stresses rising with an increase of the strain rate.
- The dynamic increase factors of spruce wood in the longitudinal, tangential, and radial direction were obtained.
- The dynamic increase factors of teak wood in the longitudinal and radial direction were obtained.
- The parameters applied in the numerical simulation using LS-Dyna for the SHPB rods, the tested wood materials and the contacts in the experiments conducted were satisfactory.

Abstract. Spruce and teak wood as anisotropic materials have complex behavior, particularly in the relationship between strain-rate and strength. High strain-rate compression tests between 590 s^{-1} and 3300 s^{-1} were carried out using two types of split Hopkinson pressure bar (SPHB) in order to measure the behavior of the wood along three principal axes with respect to fiber direction and growth rings. Numerical simulation using finite element software of the wood materials under high strain rates was performed and showed results with only a difference of 10% to the experimental results. The strain rate affects the strength of materials. In this case, it follows the power function, which means the higher the strain rate, the stronger the material.

Keywords: *compressive load; finite element; high strain rate; mechanical behavior; split Hopkinson pressure bar; spruce and teak wood.*

1 Introduction

Wood has been widely used as a construction material throughout history. However, it is still difficult to understand the mechanical properties of wood, under dynamic loading in particular, considering the variety of wood materials. In the existing literature, only few investigations have been performed using a split Hopkinson pressure bar. Data on the mechanical properties of wood are

Received March 16th, 2020, 1st Revision July 14th, 2020, 2nd Revision August 8th, 2020, Accepted for publication September 17th, 2020.
 ISSN: 2337-5779, DOI: 10.5614/j.eng.technol.sci.2021.53.1.3

mostly only available under static loading conditions. Moreover, Indonesian teak wood has not been investigated yet, particularly to obtain the dynamic increase factor (DIF); most researches were conducted on European wood types. These previous researches did not provide adequate information about wood mechanical properties under dynamic loading, which is very important for further research related to dynamic and impulsive loadings, such as blast and impact analyses.

Becker [1] classifies strain rate tests into 5 categories, i.e. creep, static, dynamic, high-speed impact, and hypervelocity impact tests. Widehammar [2] investigated wood under low (8×10^{-3} s^{-1}), medium (17 s^{-1}), and high (1000 s^{-1}) strain rate compressive loading. The results were stress-strain relationships for each fiber direction at a variety of moisture levels and strain rates. Harrigan, *et al.* [3] found that when a cellular material is impacted at high velocity, a plastic shock wave will propagate through the material, which leads to an increase of the collapse strength of the material. This increment can be quantified using a simple one-dimensional shock model. Tagarielli, *et al.* [4] concluded that for a typical PVC foam (Divinycell H250) the shock wave propagation effects are important for compression velocities $v > 60$ m s^{-1}. Tagarielli limited the velocity to less than 20 m s^{-1} and hence expected that shock wave propagation plays only a minor role in governing the dynamic response of cellular materials. The experimental data for compressive strength as a function of strain rate fit the power law. The compressive yield strength of H250 PVC foam and LD7 balsa wood doubled when the strain rate was increased from quasi-static rates (10^{-4} s^{-1}) to rates in the order of 10^{-3} s^{-1}. In contrast, H100 PVC foam showed only a small elevation in uniaxial compressive strength (about 30%) for the same increase in strain rate.

Previous researchers have observed that the fiber structure of wood and the hydrophilic nature of cellulose determine the dispersion of moisture, which is important because moisture affects the stress-strain relationship apart from the mechanical properties of wood. Renaud [5] conducted a high strain rate compressive test on 3 types of wood, i.e. aspen, birch, and oak in dry and wet conditions using water, glycerol, and hexane. He concluded from the experiment that woods with high moisture content have higher strength under high strain rate loading. Allazadeh and Wosu in [6] investigated the dynamic failure of dry maple wood with two varieties of thickness to survey the effect of dimension on wood material behavior under high strain rate failure. They concluded that when the specimen thickness is doubled, the strain rate increases fourfold and greater strains are produced during higher energy events. Maillot in [7] investigated balsa wood using LS-DYNA. Maillot compared two models of materials, i.e. wood (MAT_142) and honeycomb (MAT_026). Both materials were examined under compression, tension, hydrostatic, and shear loading. It was revealed that MAT_026 matched the experimental results, while MAT_142 showed a considerable gap under stress and shear loading.

The present research was undertaken to investigate the relationship between strain rate and strength of Norwegian spruce wood and Indonesian teak wood in various loading directions, i.e. longitudinal, tangential and radial for the spruce, while the teak was tested for its longitudinal and tangential directions, using a split Hopkinson pressure bar. The dynamic increase factor of each wood specimen was also examined. The experimental result was then used to develop a numerical model of wood material behavior under high strain-rate loading conditions using a finite element model in LS-DYNA.

2 Experimental Investigation

2.1 Specimens

The wood specimens used in this experiment were Norwegian spruce wood (*Picea Abies*) and Indonesian teak wood (*Tectona Grandis*). The geometrical shape of a cylinder was applied to avoid structural and geometric effects. Pankow, *et al.* [13] showed that experimental responses have a strong correlation with the length-diameter ratio of the specimens. According to Hou [8], the representative elementary volume (REV) in each direction of the specimen should have a minimum of 6- or 7-unit cells. Wouts [9] states that the minimum length for the longitudinal direction is 24-28 mm and 12-14 mm for soft and hard wood respectively, while a minimum of 0.3 mm and 0.15 mm length is required for the tangential direction of soft and hard wood respectively. Furthermore, the length-diameter ratio of the specimens was 1:2, considering the non-buckling indication. In this research, spruce was classified as a soft wood while teak was classified as a hard wood. The water content of the specimens was measured. The results were between 8% and 10%. The dimensions of the specimens used in the experiment are shown in Figure 1.

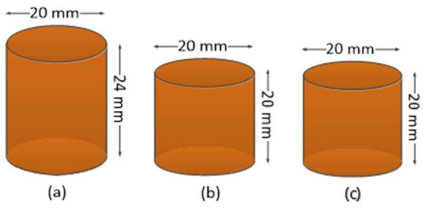

Figure 1 The spruce wood specimen dimensions for the (a) longitudinal (b) and the tangential loading direction, and the teak wood specimen dimensions (c).

2.2 Split Hopkinson Pressure Bar

In general, an SHPB consists of three components, i.e. a loading device, bar components, and a data recorder and receiver system. A schematic depiction of

the SHPB can be seen in Figure 2(a) and (b). The loading device consists of a shooter that is composed of a pressure tank, a pipe, and a striker bar. There are two rod components, i.e. an incidence bar and a transmitter bar, which should remain elastic. The ratio between the length (L_b) and the diameter (D_b) of each bar is 50. Each bar, including the striker bar, has the same diameter of 25 mm. This is larger than the diameter of specimens with a ratio of 80%. A minimum striker length (L_{bs}) of 30%Lb is required, therefore, a 375-mm long striker was used.

For the teak wood investigation in the longitudinal and in the tangential direction steel was used for the rod components. Steel was also used for the spruce wood in the longitudinal direction. Acrylic material was used for the rod components for the spruce investigation in the tangential and the radial direction.

Table 1 Bar dimensions.

Section	Length (mm)	Diameter (mm)
Striker bar	375	25
Incidence bar	1250	25
Transmission bar	1250	25

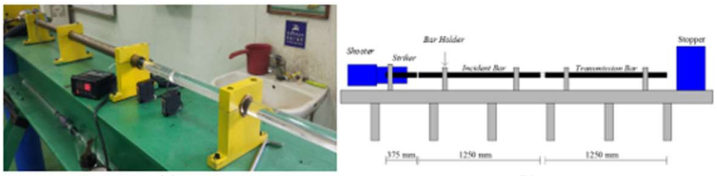

Figure 2 The Split Hopkinson pressure bar: (a) experimental setup, (b) scheme.

The SHPB works as follows: first, pressurized air is shot into the pounding bar by the shooter of the loading device. Then the pressure wave that occurs in the striker bar propagates to the incidence bar. When it reaches the specimen, the pressure wave will propagate into a wave that is forwarded to the transmission bar and into a reflected wave that is returned to the incidence bar. A strain gauge to measure the occurring strain is placed in the middle span of both the incidence bar and the transmission bar, as can be seen in Figure 3. Strain signals from the strain gauge are received by a Wheatstone bridge and then the signals are magnified by an amplifier. The magnified signals are recorded by a data acquisition system. The recorded signals are used to calculate the strain rates ($\dot{\varepsilon}$), strains (ε), and stresses (σ) of the specimen. The following equations were used to calculate the desired material properties [10]:

$$\dot{\varepsilon}(\mathrm{t}) = 2\frac{C_0}{Ls}\varepsilon_R(t) \tag{1}$$

$$\varepsilon(t) = 2\frac{C_0}{Ls}\int_0^t \varepsilon_R(t)dt \quad (2)$$

$$\sigma(t) = E\frac{A_0}{A}\varepsilon_T(t) \quad (3)$$

where C_0 is the wave velocity in the bar, Ls is the specimen length, E is the bar elasticity modulus, A_0 is the cross-sectional area of the bar, A is the cross-sectional area of the specimen, ε_R is the strain reflected on the incidence bar, and ε_T the forwarded strain on the transmission bar. In this experiment, high strain rates of approximately 590 s^{-1} to 3300 s^{-1} were applied.

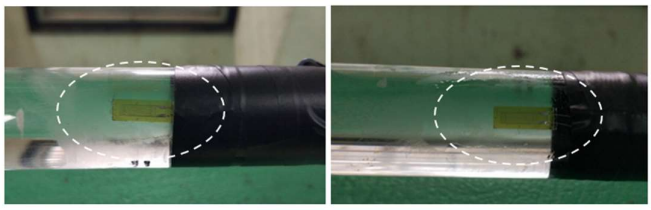

(a) (b)

Figure 3 Strain gauges in the middle span of (a) the incidence bar and (b) the transmission bar.

3 Experimental Investigation Result

3.1 Static Investigation

The overall static testing of the teak wood revealed that the mean MOE was 11461.6 MPa for the longitudinal direction and 606.8 MPa for the tangential direction. The average yield strength (σ_y) was 45.60 MPa and 6.38 MPa for the longitudinal direction and the tangential direction respectively (See Table 2).

Table 2 Static investigation results for teak wood.

Specimen	Dimension (mm)	E (MPa)	Average E (MPa)	σ_y (MPa)	Average σ_y (MPa)
JLS-01	50x50x200	9091.3	11461.6	45.10	45.60
JLS-02	50x50x200	9000.1		42.90	
JLS-03	50x50x200	13761		45.58	
JLS-04	50x50x200	13994		48.83	
JTS-01	50x50x150	652.9	606.8	6.40	6.38
JTS-02	50x50x150	587.7		7.20	
JTS-03	50x50x150	583.83		5.64	
JTS-04	50x50x150	603.13		6.27	

The overall static testing of the spruce wood showed that the mean MOE was 1908.99 MPa for the longitudinal direction, 118.2 MPa for the tangential direction, and 113.4 MPa for the radial direction. The average yield stress (σ_y) was 42.04 MPa, 5.60 MPa, and 4.48 MPa for the longitudinal, tangential, and radial loading direction respectively (See Table 3).

Table 3 Static investigation results for spruce wood.

Specimen	E (MPa)	Average E (MPa)	σ_y (MPa)	Average σ_y (MPa)
SLS-01	1853.55		43.75	
SLS-02	2024.97	1908.99	43.70	42.04
SLS-03	1848.45		38.69	
STS-01	89.725		4.96	
STS-02	142.47	118.23	6.27	5.60
STS-03	122.49		5.57	
SRS-01	130.36		5.39	
SRS-02	100.53	113.40	3.90	4.48
SRS-03	109.37		4.15	

3.2 Dynamic Investigation Using SPHB

The tests were carried out on 5 types of specimens with the loading axes following the three principal axes of wood with respect to fiber direction and growth rings, as shown in Figure 4, i.e. longitudinal direction spruce, tangential direction spruce, radial direction spruce, longitudinal direction teak, and tangential direction teak.

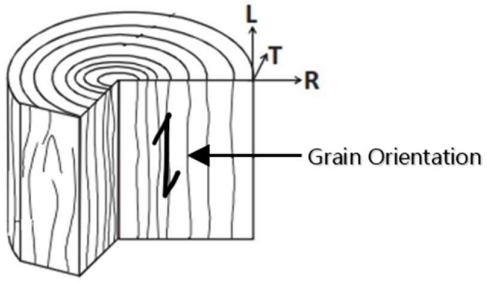

Figure 4 Three loading axes of wood with respect to fiber direction and growth rings, i.e. longitudinal (L), tangential (T) and radial (R).

The test on the longitudinal direction spruce wood was performed using a collision speed in the range of 30 to 60 m/s in Figure 5(a). At that speed, the strain rate was between 1936.43 s^{-1} and 3387.22 s^{-1} with the yield stress (σ_y) ranging from 134.26 MPa to 498.67 MPa. Testing of the spruce wood for the tangential direction was done using a striker bar speed of 35-90 m/s, which gave a strain

rate value varying from 590.79 s^{-1} to 2529.51 s^{-1} and stress values varying from 5.43 MPa to 68.33 MPa in Figure 5(b).

The third direction test on spruce wood in Figure 6, for the radial direction, was executed with a bar striker speed of 40-100 m/s. The ranges of strain rate and stress value were from 931.42 s^{-1} to 2998.74 s^{-1} and from 6.19 MPa to 58.64 MPa, respectively. In the experiment with the teak wood for the tangential direction, the striker bar speed reached 30-55 m/s with the strain rate between 1909.49 s^{-1} and 3234.56 s^{-1}, and the stress varying from 55.53 MPa to 235.06 MPa. A striker bar speed from 20 m/s to 70 m/s was provided to investigate the teak wood along the longitudinal direction. A range of strain rate from 1914 s^{-1} to 3835.32 s^{-1} and a range of stress from 189.14 MPa to 471.63 MPa were obtained.

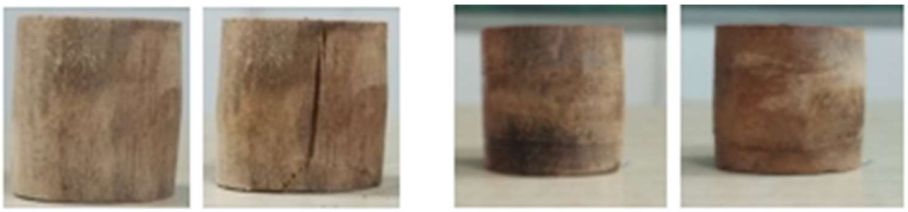

(a) (b)

Figure 5 Teak wood specimens before (left) and after (right) collision along the (a) longitudinal direction and (b) tangential directions.

(a) (b) (c)

Figure 6 Spruce wood specimens before (left) and after (right) collision along the (a) longitudinal, (b) tangential and (c) radial directions.

3.3 Dynamic Increase Factor (DIF)

The dynamic increase factor of the investigated materials can be obtained from the static and dynamic tests carried out. The DIF of the spruce was between 5.8 and 7.8 under longitudinal loading for a range of strain rates from 1936 s^{-1} to 3387 s^{-1}, between 2.0 and 6.0 under tangential loading for a range of strain rates from 591 s^{-1} to 2530 s^{-1}, and between 4.0 and 6.0 under radial loading for a range of strain rates from 931 s^{-1} to 2999 s^{-1}, as shown in Figure 7.

For the teak wood, as shown in Figure 8, the DIFs for longitudinal and tangential loading were from 20 to 25 and 4.0 to 6.5, respectively. The strain rates responsible for these DIF values were between 1914 s^{-1} and 3835 s^{-1} for longitudinal loading and between 1910 s^{-1} and 3235 s^{-1} for tangential loading.

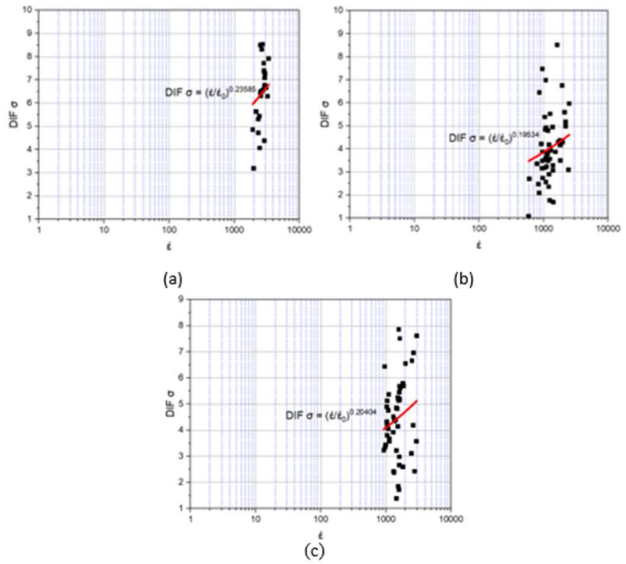

Figure 7 The relationship between strain rate and DIF stress of spruce wood on a log scale for the (a) longitudinal, (b) tangential and (c) radial direction.

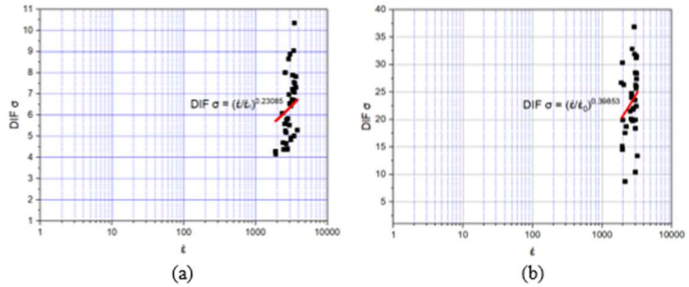

Figure 8 The relationship between strain rate and DIF stress of teak wood on a log scale from the (a) longitudinal and (b) tangential direction.

As can be seen in Figures 7 and 8, the data reveal the relationship between the measured DIFs of stresses and strains. The relationship was approached using the power law, as shown in Eq. (4):

$$DIF = \frac{\sigma_{pl}}{\sigma_0} = \left(\frac{\dot{\varepsilon}}{\dot{\varepsilon}_0}\right)^m \quad (4)$$

where m is the power law exponent, σ_{pl} and $\dot{\varepsilon}$ are the measured stress and strain respectively, σ_0 and $\dot{\varepsilon}_0$ are the reference stress and strain fit to the experimental data, providing the coefficients and m. The reference strain rate was $\dot{\varepsilon}_0 = 1\ s^{-1}$. The power law coefficient to fit the experimental data obtained is described in Table 4.

Table 4 Power law coefficient to fit the experimental data.

Type of wood	Loading Direction	σ_0 (MPa)	m
Spruce	Longitudinal	42.0	0.236
	Tangential	5.6	0.195
	Radial	4.5	0.204
Teak	Longitudinal	45.6	0.231
	Tangential	6.4	0.399

4 Numerical Model

A finite element simulation was applied in the SHPB measurement process. The details of the SHPB bar components are given in Table 1. The finite element analysis was performed using the LS-DYNA program. The striker bar, incidence bar and transmitter bar were modeled as an elastic material (MAT001) because they are required to remain elastic when the wood specimen is modeled as a honeycomb material (MAT026).

In order to obtain the stress-strain relationship of wood under high strain rate loading using an SPHB in a numerical model, the initial stress on the bar components is required. In the actual condition this stress is generated by the striker bar, which then collides with the incidence bar. A boundary condition is assigned to the end of the transmission bar to simulate the actual condition, where a stopper is placed without any distance between the transmission bar and the stopper in order to prevent the bar from moving.

The bars and the specimens are solid cylinders. Contact between the bar components because of collision occurs at the striker bar–incidence bar, the incidence bar–specimen, and the specimen–transmission bar. These cases are generally simulated using automatic surface-to-surface contact. This automatic contact type is recommended in LS-DYNA, as this type of contact is non-oriented penalty-based contact. However, this kind of assumption could cause one of the colliding bars to pierce into one another. To prevent this from happening, Afdal, *et al.* in [11] suggested constraint nodes to the surface formulation combined with the automatic surface-to-surface contact type. The bars' input parameters are provided in Table 5. A previous study conducted by Alawudin, *et al.* [12]

indicated that the mesh size of the numerical model should be sufficiently fine to produce a desirable convergence level; a convergence test should be done to verify this.

The modulus of elasticity from both woods in the longitudinal direction is provided for uncompressed and compressed conditions. The modulus of elasticity that is obtained in a state where wood is experiencing densification is called a compressed condition. A characteristic of this condition is that the modulus of elasticity suddenly rises after plastic or elastic buckling of the wood. Meanwhile, an uncompressed condition is the condition before plastic or elastic buckling.

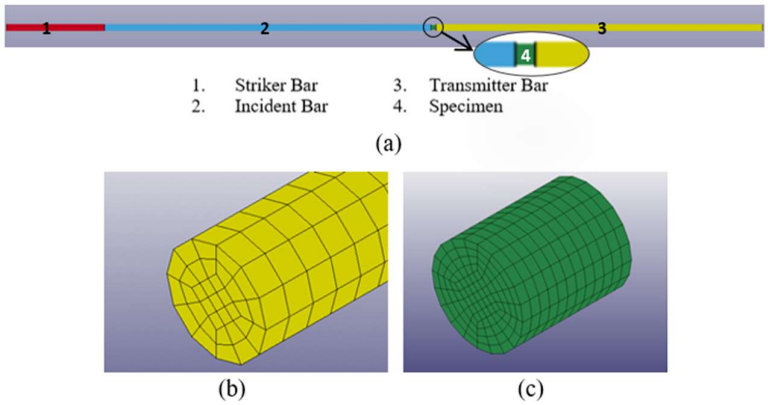

Figure 9 (a) Details of SHPB in LS-Dyna; (b) bar meshing; (c) specimen meshing.

Table 5 Input parameters.

Parameter	PMMA	Steel
ρ (kg/mm3)	1.19E-06	7.85E-06
E (GPa)	3.215	200
υ	0.3275	0.3

Table 6 Spruce wood and teak wood input data.

Data	Specimen 1	Specimen 2	Specimen 3	Loading Direction
$E_{uncompress}$	3438 MPa	8706 MPa	14508 MPa	Spruce longitudinal
$E_{compress}$	1247 MPa	2483 MPa	6254 MPa	Spruce longitudinal
$E_{uncompress}$	1325 MPa	689 MPa	842 MPa	Spruce tangential
$E_{uncompress}$	1137 MPa	432 MPa	373 MPa	Spruce radial
$E_{uncompress}$	12597 MPa	2536 MPa	6997 MPa	Teak longitudinal
$E_{compress}$	4009 MPa	3139 MPa	7475 MPa	Teak longitudinal
$E_{uncompress}$	1946 MPa	4017 MPa	3690 MPa	Teak tangential

The Young modulus for the wood modeling of the input parameters in LS-DYNA was taken from the experimental data shown in Table 6. A comparison between the results obtained in the numerical and the experimental model can be seen in Figures 10 and 11. Slightly different values of stress between the numerical model and the experimental model were observed, i.e. approximately 1%-5% for the spruce wood, i.e. 3.34%, 1.51%, and 4.36% for longitudinal, tangential, and radial loading respectively, as shown in Table 7. As for the teak wood, the difference in values obtained between the numerical and the experimental model were smaller, i.e. 2.92% for longitudinal and only 1.03% for tangential loading, as shown in Table 8.

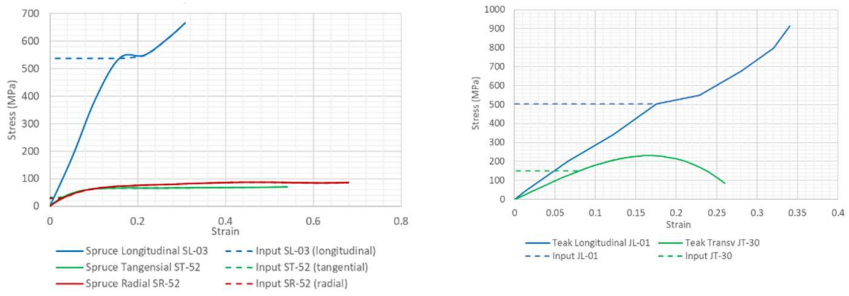

(a) (b)

Figure 10 Input curves: (a) spruce wood, (b) teak wood.

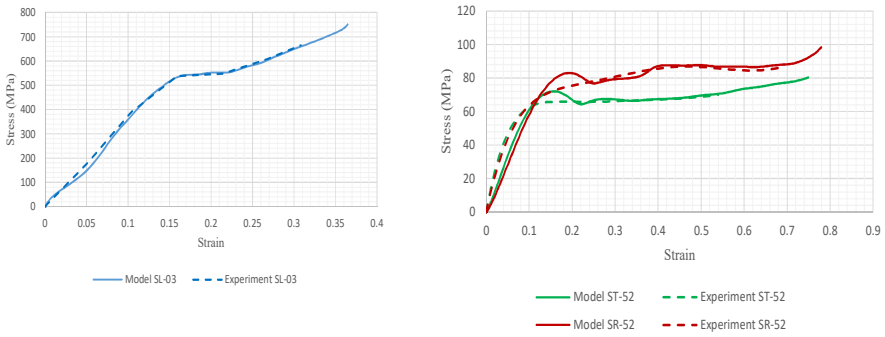

(a) (b)

Figure 11 Comparison between the model and the experiment for spruce wood for (a) longitudinal, (b) tangential and radial loading.

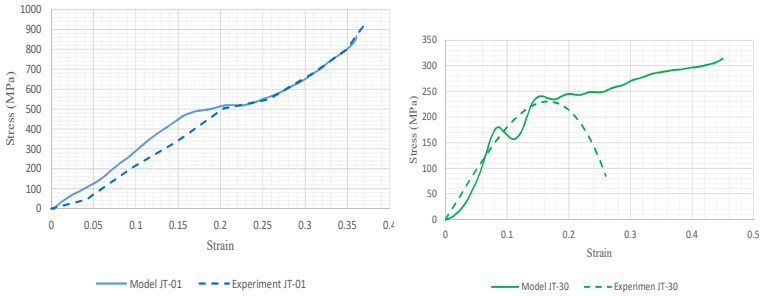

(a) (b)

Figure 12 Comparison between the model and the experiment for teak wood for (a) longitudinal and (b) tangential loading.

Table 7 Comparison between model and experiment for spruce wood.

Spruce Longitudinal		
Parameter	**Experiment**	**Model SL-03**
Collision Speed (m/s)	53	75
Yield Stress (MPa)	538.06	575.28
Yield Stress Deviation	3.34%	
Strain Rate (/s)	2600	2500
Spruce Tangential		
Parameter	**Experiment**	**Model ST-52**
Collision Speed (m/s)	61	95
Yield Stress (MPa)	33.38	34.41
Yield Stress Deviation	1.01%	
Strain Rate (/s)	2400	2400
Spruce Radial		
Parameter	**Experiment**	**Model SR-52**
Collision Speed (m/s)	96	105
Yield Stress (MPa)	29.83	32.55
Yield Stress Deviation	3.08%	
Strain Rate (/s)	2500	2500

Table 8 Comparison between model and experiment for teak wood.

Teak wood Longitudinal		
Parameter	**Experiment**	**Model JL-01**
Collision Speed (m/s)	44	65
Yield Stress (MPa)	502.53	532.77
Yield Stress Deviation	2.92%	
Strain Rate (/s)	2600	2500
Teak wood Tangential		
Parameter	**Experiment**	**Model JT-30**
Collision Speed (m/s)	48	68
Yield Stress (MPa)	150.02	146.95
Yield Stress Deviation	1.03%	
Strain Rate (/s)	2900	3000

The yield stress of the wood specimens shown in Tables 7 and 8 was calculated using bilinear approximation from the stress and strain curves. The curves were

determined from the experimental and numerical analysis as shown in Figures 11 and 12.

5 Conclusion

It can be concluded from the experiment and the numerical analysis that the stresses on teak wood and spruce wood rise by the increase of the strain rate, which indicates the dynamic increase factor phenomenon in both materials. The average used strain rates ranged from 590 s^{-1} to 3300 s^{-1}.

The DIF of spruce wood in the longitudinal direction was between 5.8 and 7.8, while for tangential and radial loading the DIFs ranged from 2.0 to 6.0 and from 4.0 to 6.0 respectively. The DIFs for longitudinal and tangential loading of teak wood ranged from 20 to 25 and from 4.0 to 6.5 respectively. Due to the high diversity of wood materials, research on wood mechanical properties, in dynamic particularly, should be carried out using more samples to obtain results that can generally represent the properties of wood.

Since wood is characterized by a complex micro-structure, developing such a realistic model of wood is troublesome. However, comparing the results of experiment and numerical analysis, the parameters applied in the numerical simulation, i.e. elastic material models for SHPB rods; honeycomb material models for wood; automatic surface-to-surface, and contact constraint node-to-surface for the contact between striker bar–incidence bar, incidence bar–specimen, specimen–transmission bar to represent the split Hopkinson pressure bar, are assumed to be satisfying.

Acknowledgements

This research was mainly funded by the Research, Community Service and Innovation Program (P3MI), Bandung Institute of Technology Year 2018. Prof. Dr.-Ing. habil. Michael Kaliske of Technische Universität Dresden, Germany is gratefully acknowledged for providing the European spruce wood samples used in this research.

References

[1] Becker, W.T. & Shipley, R.J. (Eds.), *ASM Handbook: Volume 11: Failure Analysis and Prevention*, 10th Ed., ASM International, Jul. 2002.

[2] Widehammar, S., *A Method for Dispersive Split Hopkinson Pressure Bar Analysis Applied to High Strain Rate Testing of Spruce Wood*, Doctoral Thesis, Uppsala University, Sweden, 2002.

[3] Harrigan, J.J., Reid, S.R. & Peng, C., *Inertia Effects in Impact Energy Absorbing Materials and Structures,* International Journal of Impact

Engineering, **22**(9), pp. 955-979, 1999. DOI: 10.1016/S0734-743X(99)00037-8.

[4] Tagarielli, V.L., Deshpande, V.S. & Fleck, N.A., *The High Strain Rate Response of PVC Foams and End-grain Balsa Wood*, Science Direct Part B, **39**(1), pp. 83-91, 2008.

[5] Renaud, M., Rueff, M. & Rocaboy, A.C., *Mechanical Behaviour of Saturated Wood under Compression, Part 1: Behaviour of Wood at High Rates of Strain*, Wood Science and Technology, **30**, pp. 153-164, 1996. DOI: 10.1007/BF00231630

[6] Allazadeh M.R. & Wosu S.N., *High Strain Rate Compressive Tests on Wood*, Strain **48**(2), pp. 101-107, January 2011. DOI: 10.1111/j.1475-1305.2010.00802.x

[7] Maillot, T., Lapoujade, V., Grippon,E.,Toson, B., Bardon, N. & Pesque, J.-J., *Comparative Study of Material Laws Available in LS-DYNA® to Improve the Modeling of Balsa Wood,* 13th International LS-DYNA Users Conference, Michigan, United States, 2014.

[8] Hou B., *Dynamic Enhancement and Multi-axial Behavior of Honeycombs Under Combined Shear-Compression,* PhD thesis, École Normale Supérieure de Cachan-ENS Cachan, Northwestern Polytechnical University, France, 2011.

[9] Wouts, J., Haugou, G., Oudjene, M., Coutellier, D. & Morvan, H., *Strain Rate Effects on the Compressive Response of Wood and Energy Absorption Capabilities – Part A: Experimental Investigation*, Composite Structures, **149**, pp. 315-328, 2016. ISSN 0263-8223. DOI: 10.1016 /j.compstruct.2016 .03.058.

[10] Chen, W. & Song, B., *Split Hopkinson (Kolsky) Bar Design, Testing and Application*, Mechanical Engineering Series, Springer Science+Business Media, 2011. DOI: 10.1007/978-1-4419-7982-7_10

[11] Afdhal, Jusuf A., Kariem, M.A. & Gunawan, L., *Development of a Numerical Model for Simulations of Split Hopkinson Pressure Bar*, ARPN Journal of Engineering and Applied Sciences, **11**(10), pp. 6657-6662, 2016.

[12] Awaludin, A., Irawati, I.S. & Shulhan, M.A., *Two-dimensional Finite Element Analysis of the Flexural Resistance of LVL Sengon Non-prismatic Beams*, Case Studies in Construction Materials, **10**, e00226, June 2019. DOI: 10.1016/j.cscm.2019.e00225.

[13] Pankow, M., Attard, C. & Waas, A.M., *Specimen Size and Shape Effect in Split Hopkinson Pressure Bar Testing,* Journal of Strain Analysis for Engineering Design, **44**, pp. 689-698, 2009.